**Jurnal Ilmu Fisika**
Vol. 18, No. 1, March 2026, pp. 93–104
ISSN: 1979-4657 (Print); 2614-7386 (Online)
https://doi.org/ 10.25077/jif.18.1.93-104.2026

Jurnal Ilmu Fisika
Open Access

# Hierarchical Tissue-Based MRI Features with Explainable Machine Learning for Alzheimer's Disease Classification

**Muhammed B Ceesay, Adhi Harmako Saputro, Syahril Siregar***

Department of Physics, Faculty of Mathematics and Natural Sciences, Universitas Indonesia, Depok, 16424, Indonesia.

**Article Info**

***Article History:***

Received January 26, 2026
Revised February 19, 2026
Accepted February 28, 2026
Published online March 01, 2026

***Keywords:***

*Alzheimer's disease*
*Cerebrospinal fluid*
*Hierarchical tissue atrophy*
*Machine learning*
*MRI biomarkers*

**Corresponding Author:**

Syahril Siregar
Email: syahril.siregar@ui.ac.id

**ABSTRACT**

Alzheimer's disease (AD) is a progressive neurodegenerative disorder characterized by multiscale structural brain degeneration. Many MRI-based machine learning approaches rely on coarse volumetric measures or black-box models with limited anatomical interpretability. This study aims to localize anatomically meaningful brain regions that discriminate AD from cognitively normal (CN) subjects using a hierarchical tissue-based (HTB) MRI framework. The method models gray matter (GM), white matter (WM), and cerebrospinal fluid (CSF) volumetric changes at lobar, gyral, and 246 fine-grained subregions defined by the Brainnetome atlas. T1-weighted MRI scans from 454 participants (227 AD, 227 CN) obtained from ADNI and MIRIAD were preprocessed using AC-PC alignment, N4 bias correction, skull stripping, and nonlinear registration to MNI space. A total of 561 HTB features were extracted to train Random Forest and XGBoost classifiers using five-fold stratified cross-validation with Bayesian hyperparameter optimization. The XGBoost model achieved the best performance (Accuracy: 79.74%, ROC-AUC: 85.07%), comparable to recent atlas-based MRI classification studies, while providing improved multiscale anatomical interpretability. SHAP analysis revealed consistent hierarchical atrophy patterns in hippocampal subregions, medial amygdala, and areas 35/36 and 28/34, demonstrating that hierarchical anatomical modeling with explainable machine learning enables transparent localization of clinically meaningful AD biomarkers without reliance on black-box architectures.



## 1. INTRODUCTION

Alzheimer's disease (AD) is a progressive neurodegenerative disorder characterized by extracellular beta-amyloid (Aβ) plaque deposition and intracellular neurofibrillary tangles composed of hyperphosphorylated tau proteins. Clinically, AD primarily presents with memory impairment, although deficits in speech, spatial awareness, and decision-making are also common (Zhou et al., 2026). The hippocampus plays a crucial role in memory formation and consolidation; therefore, early neuronal dysfunction in this region leads to memory impairment and difficulty in forming long-term memories (Muthuchetty, 2026). As the leading cause of dementia, AD is among the costliest and most disabling diseases worldwide. Approximately 50 million people currently live with dementia, and this number is

projected to reach 100–130 million by 2040–2050, with about 70% of cases attributed to AD (Scheltens et al., 2021). Despite extensive advances in basic and clinical research, the absence of effective preventive or curative therapies continues to pose a major global health challenge (Wijeratne et al., 2023).

Artificial intelligence (AI) methods aim to identify optimal models that best represent complex datasets. Machine learning (ML), a subset of AI, offers advantages such as non-linearity, fault tolerance, and real-time processing, making it well-suited for complex biomedical applications (Chang et al., 2021). Over the years, ML has shown considerable promise for the early identification and classification of AD using neuroimaging data (Sorour et al., 2024). Among multimodal neuroimaging techniques, magnetic resonance imaging (MRI) is widely used due to its ability to capture complementary pathological signatures. Neuroimaging data are traditionally categorized into gray matter (GM), white matter (WM), and cerebrospinal fluid (CSF), and extensive evidence suggests that volumetric changes in these tissue compartments are closely associated with AD severity. Accordingly, prior studies have employed GM volume, combinations of multi-tissue features, or whole-brain volumetric measures as inputs to ML and deep learning models to improve diagnostic accuracy (Khojaste-Sarakhsi et al., 2022; Xu et al., 2023).

Most existing MRI-based ML studies primarily rely on whole-brain GM volumes or single-scale regional features derived from conventional atlases, with the primary objective of maximizing classification accuracy. Such approaches typically treat anatomical regions independently and do not explicitly model the hierarchical organization of brain structures, thereby limiting their ability to characterize progressive, multiscale atrophy patterns. Even atlas-based methods, including those using fine-grained parcellations, generally employ features at a single anatomical resolution without integrating lobar, gyral, and subregional levels within a unified framework.

The primary objective of this study is therefore not merely to maximize classification accuracy, but to localize and hierarchically characterize anatomically meaningful brain regions that most strongly discriminate AD from cognitively normal (CN) subjects. To achieve this, we propose a hierarchical tissue-based (HTB) MRI framework that models GM, WM, and CSF volumetric alterations at lobar, gyral, and 246 fine-grained subregional levels defined by the Brainnetome atlas. This multiscale representation enables systematic investigation of structural degeneration patterns in a manner consistent with the known hierarchical progression of AD pathology.

Unlike non-hierarchical volumetric approaches and non-interpretable ML models, the proposed framework integrates Extreme Gradient Boosting (XGBoost) and Random Forest (RF) with SHapley Additive exPlanations (SHAP) analysis aimed at identifying key brain regions that exhibit the most discriminative biomarkers of AD across multiple anatomical scales. By modeling volumetric tissue atrophy at the lobar, gyral, and fine-grained subregional levels, as defined by the Brainnetome atlas, the proposed approach enables investigation of AD-related structural changes in a manner that reflects the progressive nature of the disease. The Brainnetome atlas provides a high-resolution, connectivity-based parcellation of the brain into 246 fine-grained subregions, allowing detailed characterization of localized atrophy patterns. This hierarchical tissue-based representation facilitates comprehensive assessment of AD-related structural alterations and supports the identification of region-specific biomarkers. This combination allows quantitative ranking and transparent localization of discriminative brain regions and tissue features that drive model predictions. By explicitly linking multiscale anatomical features to interpretable ML outputs, the framework facilitates the identification of biologically meaningful biomarkers aligned with established neuropathological evidence.

## 2. METHOD

### 2.1 Data Collection

The data used in the proposed study consist of two publicly accessible databases, namely, the Alzheimer's Disease Neuroimaging Initiative (ADNI) database and the Minimal Interval Resonance Imaging in Alzheimer's Disease (MIRIAD) database, to enhance variability, robustness, and

generalizability across imaging protocols. In 2003, the ADNI was initiated as a public- private collaboration led by the principal investigator Michael W. Weiner, and the main aim of the study was to determine whether serial MRI, positron emission tomography (PET), other biological biomarkers, and clinical and neuropsychological measurements could be combined to monitor the course of mild cognitive impairment (MCI) and early AD. For further details, go to https://adni.loni.usc.edu/. ADNI is an extensive, longitudinal, and standardized resource, offering multimodal information: structural, functional, and molecular neuroimaging, biofluid biomarkers, genetic profiles, demographic data, and cognitive measurements, and has become among the most popular datasets to use in research and diagnostic models of AD.

MIRIAD database, which was launched in 2013, contains longitudinal T1-weighted volumetric MRI scans obtained from 46 patients with Alzheimer's and 23 cognitively normal (CN) subjects. The total number of MRI scans in the dataset is 798 scans at specified intervals (0, 2, 6, 14, 26, 38, and 52 weeks) with the same imaging equipment, which allows performing longitudinal analysis. Besides the imaging data, MIRIAD offers demographic and clinical data, such as age, sex, and the Mini-Mental State Examination (MMSE) scores, which allow performing a profound analysis of the disease progression by means of an image-based analysis exclusively (Malone et al., 2013).

Overall, the study used T1-weighted MRI images acquired using a Modified Magnetization-Prepared Rapid Gradient Echo (MPRAGE) sequence at 1.5T from a total of 454 participants, in which 227 subjects are cognitively normal, and 227 patients diagnosed with AD. Among them, 204 CN and 181 AD samples were obtained in the ADNI database, and 23 CN and 46 AD samples were obtained in the MIRIAD database.

### 2.2 Data Preprocessing

A standardized preprocessing pipeline was applied using the ANTsPy toolkit to ensure data quality and consistency prior to feature extraction and model training. All T1-weighted MRI scans were first aligned to the anterior commissure–posterior commissure (AC–PC) plane and corrected for intensity inhomogeneities using N4 bias field correction. Brain tissue was extracted using a deep learning–based skull-stripping method, followed by Gaussian smoothing ($\sigma = 1.34$) applied within the brain mask to reduce noise. Each volume was subsequently nonlinearly registered to the MNI152_T1_1mm standard template using the Symmetric Normalization (SyN) algorithm and resampled to an isotropic resolution of $1\times1\times1 mm^3$.

### 2.3 Feature Extraction

#### 2.3.1 Tissue Segmentation

The distribution of MRI voxel intensities is estimated with the employment of Gaussian Mixture Modelling (GMM), which illustrates this as a weighted summation of various Gaussian distributions, and this technique is most suitable when carrying out a brain tissue segmentation problem. Each Gaussian component describes the statistical properties of the various types of tissues. TheGaussian distribution of a vector is denoted as $N(x|\mu,\Sigma)$ in equation 1, where the mean vector is given as $\mu$, and the covariance matrix ($\Sigma$) (Binti Kasim et al., 2021; Riaz et al., 2020).

$$N(x|\mu,\Sigma) = \frac{1}{(2\pi^2)^{\frac{D}{2}}|\Sigma|^{\frac{1}{2}}} exp\left(\frac{1}{2}(x-\mu)^T\Sigma^{-1}(x-\mu)\right) \quad (1)$$

The final probability distribution P(x) is obtained by weighing each Gaussian mixture component (K) by its corresponding mixture weight ($w_j$) and summing the weighted components.

$$P(x) = \sum_{j=1}^{K} w_j N(x|\mu,\Sigma) \quad (2)$$

In this study, a three-component GMM ($K = 3$) was applied to normalized T1-weighted brain MRI volumes to model CSF, GM, and WM. Model parameters were estimated using the Expectation-

Maximization (EM) algorithm with a maximum of 300 iterations, initialized with preset mean values corresponding to the three tissue classes. Soft probabilistic tissue maps were obtained from these posterior probabilities. Hard tissue segmentation was then performed by assigning each voxel to the tissue class with the maximum posterior probability, where $C_j \in \{CSF, GM, WM\}$ denotes the tissue class as shown in equation 3.

$$\text{Label}(x) = \arg\max_{j\epsilon\{1,2,3\}} P(x|C_j) \quad (3)$$

To improve spatial coherence and reduce noise, the resulting label maps were further refined using three-dimensional morphological operations, including binary opening, closing, and hole filling.

### 2.3.2 Hierarchical Tissue-Based (HTB) Scaler Feature Extraction

ANTsPy library was utilized to obtain HTB features using the Brainnetome Atlas as an anatomical guide as described in their official website, Brainnetome Atlas | Atlas. The atlas provides a multiscale anatomical grid that includes lobar, gyral, and 246 further subregional parcellations, and this enables a systematic description of volumetric patterns of tissue atrophy regarding the pathology of AD.

The outcome of this step is a set of HTB features, which includes atrophy of the tissue at the lobar, gyral, and fine-grained subregional levels, as well as global volumetric CSF, GM, and WM features. ANTsPy was used to create brain masks of each region of interest (ROI), and the segmented GM and WM tissue probability maps were multiplied by the corresponding ROI masks to get region-specific tissue properties (see Figure 1). GM/WM and GM/CSF volumetric ratios were also calculated along with the absolute volumetric values to further explain the composition of the tissues. Generally, this process led to 561 quantitative features of HTB. These scalar properties can depict volumetric atrophy at multiple scales of the anatomy and produce interpretable indices of structural brain changes in the course of disease progression.

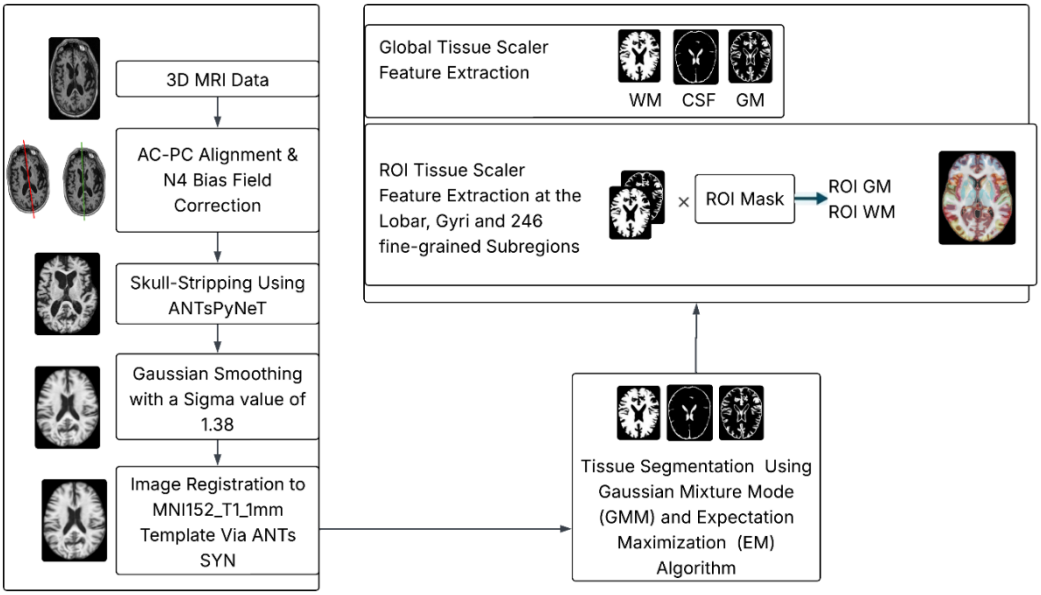


**Figure 1** Overview of the data preprocessing and HTB feature extraction workflow implemented with the ANTsPy library.

## 2.4 Model Implementation

XGBoost and RF classifiers are the distinct ML models employed in the proposed framework to distinguish AD from CN subjects (see Figure 2). All experiments were implemented in Python 3.10 using the scikit-learn library and executed in Visual Studio Code on the workstation with 12 GB of RAM space. The extracted HTB features were used to train the two classifiers, denoted as HTB

XGBoost and HTB RF. Each model was trained and evaluated independently using five-fold stratified cross-validation to provide a balanced trade-off between bias and variance for moderate sample sizes while ensuring stable performance estimation, with an internal three-fold cross-validation for hyperparameter optimization. Data splitting was done at the patient level to avoid data leakage. The features in the training pipeline were normalized using MinMaxScaler and optimized via Bayesian hyperparameter optimization in order to give optimal performance.

The tuning ranges for XGBoost and Random Forest are summarized in Table 2. A supervised feature selection strategy based on mutual information was applied to reduce dimensionality whilst retaining the most discriminative features. SelectKBest algorithm selected the features on the basis of dependency on the target variable by computing the mutual information of each feature and the class labels. The K (number of selected features) parameter was optimized in the parameter search space, resulting in 559 features out of 561 selected for both the HTB XGBoost and RF models. Further dimensionality reduction did not yield statistically significant performance improvement, indicating that aggressive feature elimination was not critical for model generalization. This is consistent with the robustness of tree-based ensemble models, which inherently perform embedded feature selection during split optimization.

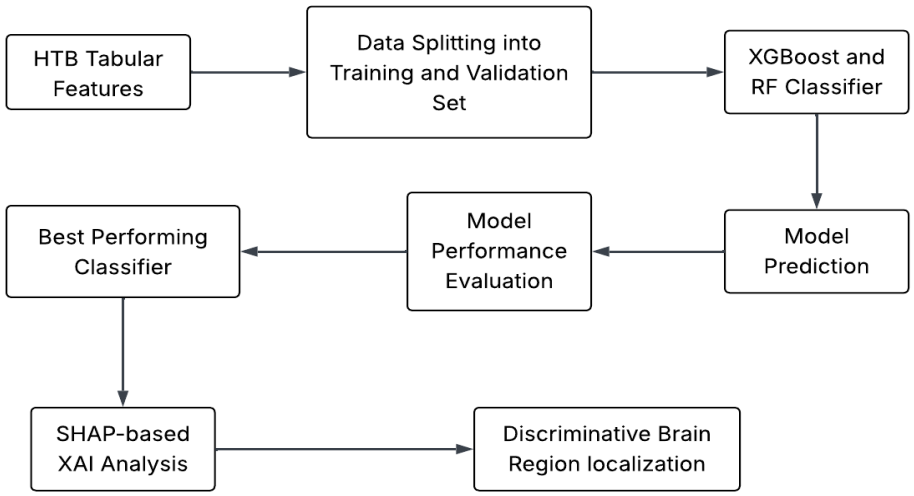


**Figure 2** Proposed classification framework with SHAP-based XAI applied to the best-performing model.

**Table 2** Hyperparameter ranges and categorical options explored during Bayesian optimization for the XGBoost and RF models.

| Model | Hyperparameter Search Space |
|---|---|
| XGBoost | n_estimators: 100–2000; max_depth: 2–8; learning_rate: 0.01–0.5 (log-uniform); subsample: 0.5–1.0; colsample_bytree: 0.5–1.0; gamma: 0.5–10.0; reg_alpha: 0–10; reg_lambda: 0–10; min_child_weight: 1–10 |
| RF | n_estimators: 100–2000; max_depth: 2–50; min_samples_split: 2–20; min_samples_leaf: 1–10; max_features: {sqrt, log2, None}; bootstrap: {True, False}; class_weight: {None, balanced} |

## 2.5 SHAP-Based Explainable AI

Explainable Artificial Intelligence (XAI) refers to techniques designed to interpret and explain the decisions and reasoning processes of artificial intelligence models, thereby enhancing transparency and trustworthiness for end-users. Most XAI methods compute feature attribution scores at the pixel or feature level to quantify the contribution of each input to model predictions (Kuroki & Yamasaki, 2024;

Truong Thanh Nguyen et al., 2021). In this study, SHAP was employed to improve the interpretability of the XGBoost classifier and to localize the most discriminative brain regions associated with AD. SHAP values were visualized using summary and dependence plots to provide global interpretations of the model's predictions (Vimbi et al., 2024). Such techniques are particularly valuable in medical applications, as they facilitate the interpretation of ML models used for AD diagnosis by quantifying the contribution of each input feature to the final prediction, enabling clinicians to identify potential early biomarkers, improve diagnostic accuracy, and support timely intervention before neurodegeneration becomes irreversible (Khanapur et al., 2024). In this work, SHAP-based XAI analysis was applied exclusively to the best-performing ML model to identify discriminative brain regions that most strongly influenced the model's decision-making process.

## 3. RESULTS AND DISCUSSION

### 3.1 Results

#### 3.1.1 Evaluation Metrics

Table 3 presents a summary performance of the proposed machine learning models in distinguishing AD from CN subjects using HTB features. Various measures of evaluation, such as accuracy, precision, recall, F1-score, Receiver operating characteristic area under the curve (ROC-AUC), and specificity, were used to evaluate the effectiveness of the proposed framework. The XGBoost classifier based on the proposed approach was able to achieve 79.74±0.022%, 80.00±0.073%, 79.30±0.061%, 79.65±0.015%, 85.07±0.016% and 80.18±0.093% in accuracy, precision, recall, F1-score, ROC-AUC, and specificity, respectively. XGBoost slightly outperformed Random Forest due to its gradient boosting mechanism, which sequentially optimizes residual errors and captures complex non-linear interactions among hierarchical tissue-based features. Its built-in regularization and learning rate control also enhance generalization when handling high-dimensional, multiscale neuroimaging data. In contrast, RF relies on independent tree averaging (Yajjala et al., 2025), which may limit its ability to fully exploit subtle hierarchical dependencies across anatomical scales. In addition, Figure 3 provides the ROC-AUC curve of the XGBoost and RF classifiers.

**Table 3** Performance evaluation metrics of the XGBoost and RF classifiers for distinguishing AD from CN subjects.

| Metrics | HTB XGBoost | HTB RF |
|---|---|---|
| Accuracy | 79.74±0.022% | 77.97±0.035% |
| Precision | 80.00±0.073% | 77.49±0.088% |
| Recall | 79.30±0.061% | 78.85±0.088% |
| F1-Score | 79.65±0.015% | 78.17±0.036% |
| ROC-AUC | 85.07±0.016% | 83.60±0.036% |
| Specificity | 80.18±0.093% | 77.09±0.127% |

#### 3.1.2 Discriminative Brain Regions

The hierarchical GM and WM patterns of atrophy found in the results of the SHAP algorithm of the XGBoost classifier demonstrate region-specific volumetric loss as an important discriminative AD characteristic. The global SHAP results, as presented in Figure 4, show the brain areas that have the greatest impact on the predictions by the model. It is important to note that the SHAP analysis ranked the caudal hippocampus (cHipp), rostral hippocampus (rHipp), medial amygdala (mAmyg), rostral area 35/36 (A35/36r), area 28/34 (A28/34), i.e., the Entorhinal cortex and the hippocampal gyrus region as the highest-ranking 20 regions related to AD. Moreover, the findings show that the gyral and fine-grained subregional features have been shown to have a stronger discriminative capability of AD classification than lobar-level regions, which highlights the significance of high-resolution anatomy characterization. These subregions are mapped on the MRI brain data as shown in Figure 5.

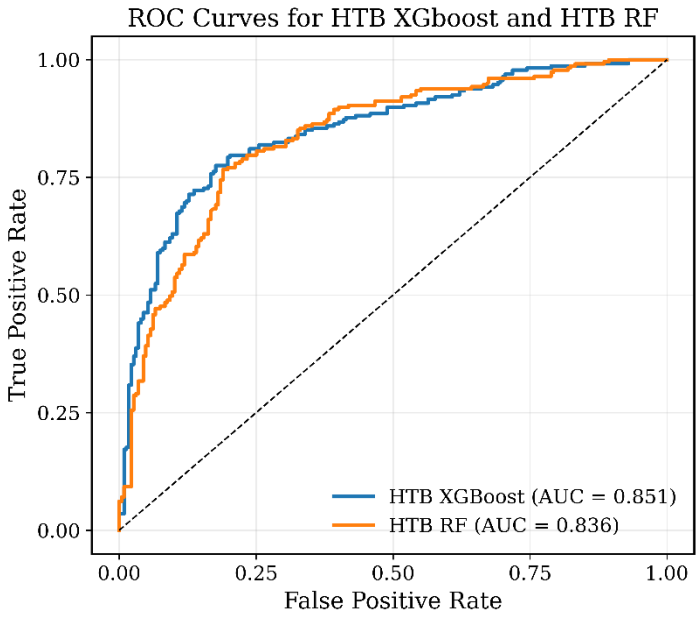


**Figure 3** illustrates the ROC-AUC curve of the XGBoost and RF model, emphasizing their capability in distinguishing AD from CN subjects.

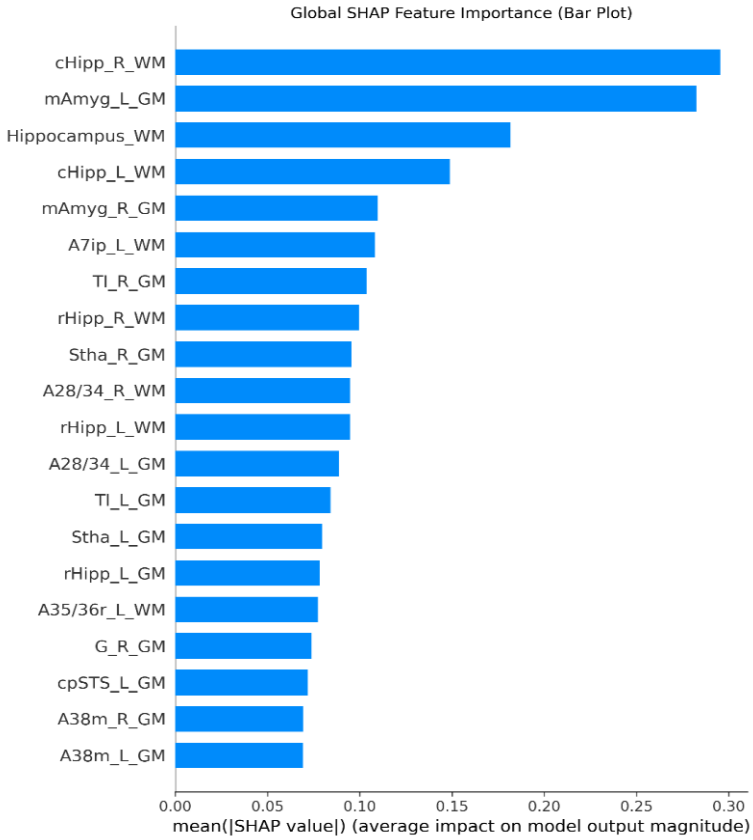


**Figure 4** Top 20 brain regions identified by SHAP, showing their relative contributions to AD vs. CN classification.

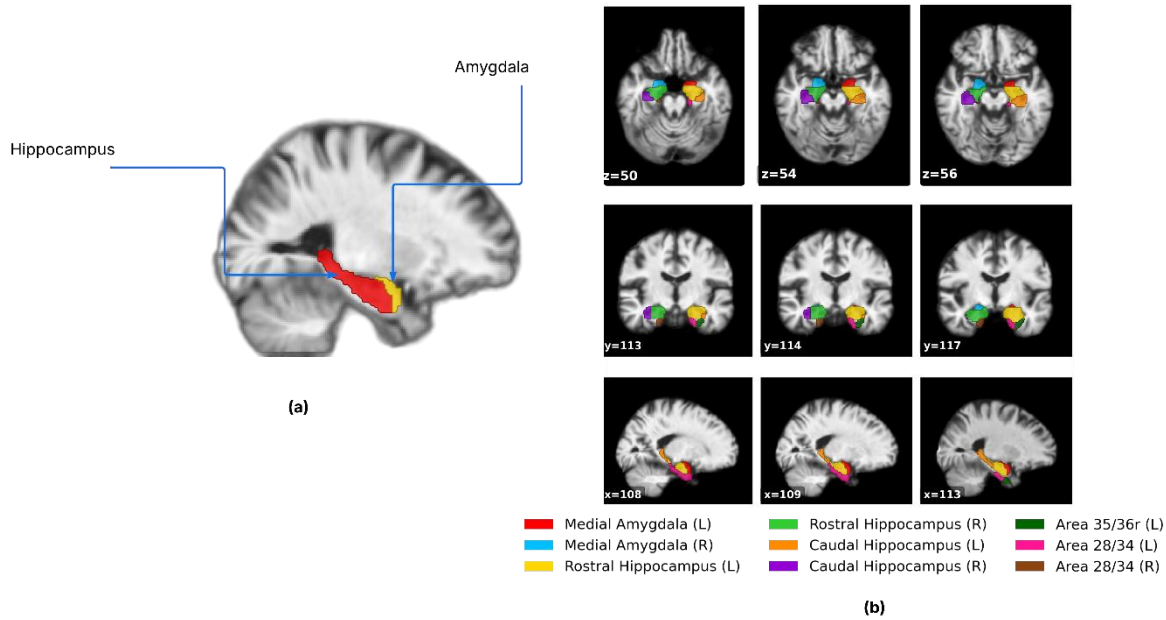


**Figure 5** Discriminative brain regions overlaid on MRI images showing (a) lobar structures and (b) Fine-grained subregional parcellations.

### 3.2 Discussion

Structural biomarkers are vital in differentiating AD from CN subjects. A clear signifier of AD is that of pronounced cortical thinning and disease-related brain atrophy, reflecting enlargement of the ventricles, which is observable in sagittal, coronal, and axial planes. Significant decreases in both GM and WM volumes are closely associated with AD progression. In particular, GM loss correlates with memory and emotional impairments and is accompanied by a compensatory increase in cerebrospinal fluid (CSF). We present a novel framework for AD classification that utilizes HTB features to characterize the multiscale progression of brain atrophy. Experimental results indicate that the HTB XGBoost classifier slightly outperforms the corresponding Random Forest (RF) model, achieving an accuracy of 79.74% compared with 77.97%. However, the primary contribution of this work lies not in maximizing classification performance, but in enabling the interpretable localization of discriminative brain regions and structural biomarkers that reflect hierarchical disease progression.

The hippocampus is a multilayered neuronal structure located in the medial temporal lobe. It plays a critical role in long-term episodic memory, spatial orientation, and higher cognitive functions such as approach–avoidance conflict resolution. The hippocampus is specifically susceptible to damage in the central nervous system due to its high plasticity. There exists significant evidence that structural and functional changes of the hippocampus are strongly linked with cognitive deficiency in significant neurodegenerative disorders, especially in AD (Hosseini et al., 2025; Hammond & Epsztein, 2024). The hippocampus is a prime and very dependable biomarker of AD according to the updated National Alzheimer's Association Diagnostic Criteria. Extensive studies have shown that the degenerative changes of the hippocampal and Aβ plaques are closely related and have been reported in various studies (Liu et al., 2022). The tau pathology first appears in the medial temporal lobe, which is in the transentorhinal cortex, and then extends to the hippocampus and amygdala. It is important to note that the amygdala develops tau tangle depositions early and severely during the preclinical stages of the disease, highlighting its significance in the early AD-related neurodegeneration (Salman et al., 2024; Schumacher et al., 2025).

In several studies, the caudal hippocampus (cHipp), rostral hippocampus (rHipp), rostral area 35/36 (A35/36r), area 28/34 (A28/34), and medial amygdala (mAmyg) have been found to be important brain subparts involved in AD. As a case in point, Equally, Pan et al also used a 3D CNN ensemble model to classify AD stages and localize discriminative brain subregions, indicating that the rostral

hippocampus, caudal hippocampus, rostral area 35/36, and medial amygdala are key regions in AD diagnosis. Their study further identified area 28/34 as a particularly informative region for distinguishing early-stage AD. (Pan et al., 2024). In the previous study, Pan et al proposed an ensemble 2D CNN system to classify AD stages and to localize the discriminative brain regions in distinguishing between AD and CN subjects. The rostral hippocampus, medial amygdala, and area 28/34 were identified as the most informative regions in AD classification (Pan et al., 2020). Similarly, Kiran et al put forward a customized dynamic ensemble convolutional neural network (PDECNN) to label AD phases through region-specific neurodegeneration and found that rostral hippocampus degeneration was frequent and pronounced in AD (Kiran et al., 2024).

Area 28/34, also known as the entorhinal cortex (EC), is a vital part of the medial temporal lobe, and it is an important center in cognitive functioning, including spatial orientation, temporal encoding, and memory formation due to its vast interconnection with the hippocampal formation. As a point of connection between the hippocampus and the neocortical areas, the EC is essential to the human memory network, and its neurons are especially susceptible to neurofibrillary inclusions. EC is one of the first areas of the cortex that develops neurofibrillary tangles in the context of AD, which include misfolded and hyperphosphorylated tau protein. Numerous stereological and neuroimaging studies have demonstrated significant neuronal loss and cortical atrophy in the EC. Importantly, these changes occur before the clinical manifestation of AD or during its earliest stages. Disturbances in memory and cognitive function have been firmly attributed to neurodegeneration in the EC and hippocampus, which, along with mounting evidence, indicates that molecular and functional degeneration of EC contributes mostly to early cognitive impairment. One of the key pathological characteristics of AD is the deposition of Aβ in the outer layers of the EC, particularly in layer II, which provides major excitatory input to the hippocampus. This accumulation is believed to trigger neurotoxic cascades that ultimately lead to substantial neuronal loss (Oltmer et al., 2022; Rani et al., 2023; Tran et al., 2022).

Areas 35 and 36 of the rostral cortical areas, which are important constituents of the perirhinal cortex, are also vital in the early phases of AD and happen to be the initial parts of the cortex to undergo the neurofibrillary tangles (NFT) pathology. Several studies reported the deposition of tau in region 35 with neural destruction and cognitive impairment, but area 36, where less well studied, shows evidence of early tau accumulation that increases with disease progression. Tau pathology in these regions is associated with reduced functional connectivity between the medial temporal lobe and cortical networks. This disruption contributes to memory deficits. It is important to note that elevated levels of tau in regions 35 and 36 are associated with minor preliminary memory issues in individuals with no cognitive impairment, but in patients with mild cognitive impairment (MCI), these elevated tau levels are coupled with severe atrophy of the regions in this group. Consistent with these results, regions 35 and 36 demonstrate significant structural degeneration at an early phase of AD, which has a strong association with cognitive dysfunction, particularly in memory-related tasks (Berron et al., 2021; Besson et al., 2020; Lu et al., 2024; Xie et al., 2020)

Importantly, our results demonstrate that gyral and fine-grained subregional features provide stronger discriminative power than lobar-level measures. This finding highlights the importance of high-resolution anatomical characterization in AD classification. Rather than treating brain regions independently or at a single anatomical scale, the HTB framework captures degeneration patterns that reflect the hierarchical organization of brain structures and the progressive nature of AD pathology.

These brain regions are critically involved in behavioral domains such as cognition, emotion, perception, memory, and language. Clinically, AD is most frequently characterized by memory impairment, progressive cognitive decline, reduced judgment, emotional instability, and language dysfunction. The outcomes of this study are consistent with prior findings and provide a reliable and biologically meaningful representation of discriminative brain regions and biomarkers associated with AD progression. Notably, the implementation of HTB features with SHAP-based explainable artificial intelligence (XAI) analysis enhances the interpretability and trustworthiness of the identified biomarkers.

## 4. CONCLUSION

This study proposed an HTB MRI framework for AD classification that models multiscale structural atrophy patterns. The HTB-XGBoost model achieved competitive classification performance while enabling anatomically interpretable biomarker localization. The major contribution of this work is that it allows for the localization of biologically significant and hierarchically consistent biomarkers of AD progression. SHAP analysis showed strong participation of hippocampal sub-regions, medial amygdala, area 35/ 36, and 28/34, which align with the known neuropathological evidence of early AD-related degeneration. These results indicate that high-resolution and hierarchical tissue structures with explainable AI are capable of providing transparent and clinically relevant information about disease mechanisms, and this appears to be a promising line of future research on the diagnostic support of AD and longitudinal studies of the progression of the disease.

## ACKNOWLEDGEMENT

This research was supported by Hibah Publikasi Pascasarjana FMIPA under contract number PKS-38/UN2.F3D/PPM.00.02/2025. M. B. C. acknowledges UI-Great scholarship for financing his study at Univeritas Indonesia.

## REFERENCE

Berron, D., Vogel, J. W., Insel, P. S., Pereira, J. B., Xie, L., Wisse, L. E. M., Yushkevich, P. A., Palmqvist, S., Mattsson-Carlgren, N., Stomrud, E., Smith, R., Strandberg, O., & Hansson, O. (2021). Early stages of tau pathology and its associations with functional connectivity, atrophy and memory. *Brain*, *144*(9), 2771–2783. https://doi.org/10.1093/brain/awab114

Besson, G., Simon, J., Salmon, E., & Bastin, C. (2020). Familiarity for entities as a sensitive marker of antero-lateral entorhinal atrophy in amnestic mild cognitive impairment. *Cortex*, *128*, 61–72. https://doi.org/10.1016/j.cortex.2020.02.022

Binti Kasim, F. A., Pheng, H. S., Nordin, S. Z. B., & Haur, O. K. (2021, September 8). Gaussian Mixture Model-Expectation Maximization Algorithm for Brain Images. *2021 2nd International Conference on Artificial Intelligence and Data Sciences, AiDAS 2021*. https://doi.org/10.1109/AiDAS53897.2021.9574309

Chang, C. H., Lin, C. H., & Lane, H. Y. (2021). Machine learning and novel biomarkers for the diagnosis of alzheimer's disease. In *International Journal of Molecular Sciences* (Vol. 22, Number 5, pp. 1–12). MDPI AG. https://doi.org/10.3390/ijms22052761

Hammond, C., & Epsztein, J. (2024). The adult hippocampal network. *Cellular and Molecular Neurophysiology*, 461–489. https://doi.org/10.1016/B978-0-323-98811-7.00005-9

Hosseini, E., Sepehrinezhad, A., Momeni, J., Ascenzi, B. M., Gorji, A., & Sahab-Negah, S. (2025). The Telencephalon: Hippocampus and Related Structures. *From Anatomy to Function of the Central Nervous System: Clinical and Neurosurgical Applications*, 401–427. https://doi.org/10.1016/B978-0-12-822404-5.00014-0

Khanapur, S., Bharadwaj, C. B., Bhardwaj, R., & Nayak, J. S. (2024). An Approach for XAI Visualizations for Explainability of Alzheimer's Detection. *Proceedings - ICNEWS 2024: 2nd International Conference on Networking, Embedded and Wireless Systems: Wireless Technology - Building a Digital World*. https://doi.org/10.1109/ICNEWS60873.2024.10731000

Khojaste-Sarakhsi, M., Haghighi, S. S., Ghomi, S. M. T. F., & Marchiori, E. (2022). Deep learning for Alzheimer's disease diagnosis: A survey. *Artificial Intelligence in Medicine*, *130*, 102332. https://doi.org/10.1016/J.ARTMED.2022.102332

Kiran, A., Alsaadi, M., Dutta, A. K., Raparthi, M., Soni, M., Alsubai, S., Byeon, H., Kulkarni, M. H., & Asenso, E. (2024). Bio-inspired deep learning-personalized ensemble Alzheimer's diagnosis model for mental well-being. *SLAS Technology*, *29*(4). https://doi.org/10.1016/j.slast.2024.100161

Kuroki, M., & Yamasaki, T. (2024). EXPLAINING 3D OBJECT DETECTION THROUGH SHAPLEY VALUE-BASED ATTRIBUTION MAP. *Proceedings - International Conference on Image Processing, ICIP*, 507–513. https://doi.org/10.1109/ICIP51287.2024.10647574

Liu, S., Jie, C., Zheng, W., Cui, J., & Wang, Z. (2022). Investigation of Underlying Association Between Whole Brain Regions and Alzheimer's Disease: A Research Based on an Artificial Intelligence Model. *Frontiers in Aging Neuroscience*, *14*. https://doi.org/10.3389/fnagi.2022.872530

Lu, F., Shi, C., Rao, D., & Yue, W. (2024). The Correlations between Volume Loss of Temporal and Subcortical Functional Subregions and Cognitive Impairment at Various Stages of Cognitive Decline. *Journal of Integrative Neuroscience*, *23*(12). https://doi.org/10.31083/j.jin2312220

Malone, I. B., Cash, D., Ridgway, G. R., MacManus, D. G., Ourselin, S., Fox, N. C., & Schott, J. M. (2013). MIRIAD—Public release of a multiple time point Alzheimer's MR imaging dataset. *NeuroImage*, *70*, 33–36. https://doi.org/10.1016/J.NEUROIMAGE.2012.12.044

Muthuchetty, S. (2026). A proposed framework for multimodal diagnosis in Alzheimer's disease. In *Discover Neuroscience* (Vol. 21, Number 1). BioMed Central Ltd. https://doi.org/10.1186/s13064-025-00227-4

Oltmer, J., Slepneva, N., Llamas Rodriguez, J., Greve, D. N., Williams, E. M., Wang, R., Champion, S. N., Lang-Orsini, M., Nestor, K., Fernandez-Ros, N., Fischl, B., Frosch, M. P., Magnain, C., Van Der Kouwe, A. J. W., & Augustinack, J. C. (2022). Quantitative and histologically validated measures of the entorhinal subfields in ex vivo MRI. *Brain Communications*, *4*(3). https://doi.org/10.1093/braincomms/fcac074

Pan, D., Luo, G., Zeng, A., Zou, C., Liang, H., Wang, J., Zhang, T., & Yang, B. (2024). Adaptive 3DCNN-Based Interpretable Ensemble Model for Early Diagnosis of Alzheimer's Disease. *IEEE Transactions on Computational Social Systems*, *11*(1), 247–266. https://doi.org/10.1109/TCSS.2022.3223999

Pan, D., Zeng, A., Jia, L., Huang, Y., Frizzell, T., & Song, X. (2020). Early Detection of Alzheimer's Disease Using Magnetic Resonance Imaging: A Novel Approach Combining Convolutional Neural Networks and Ensemble Learning. *Frontiers in Neuroscience*, *14*. https://doi.org/10.3389/fnins.2020.00259

Rani, N., Alm, K. H., Corona-Long, C. A., Speck, C. L., Soldan, A., Pettigrew, C., Zhu, Y., Albert, M., & Bakker, A. (2023). Tau PET burden in Brodmann areas 35 and 36 is associated with individual differences in cognition in non-demented older adults. *Frontiers in Aging Neuroscience*, *15*. https://doi.org/10.3389/fnagi.2023.1272946

Riaz, F., Rehman, S., Ajmal, M., Hafiz, R., Hassan, A., Aljohani, N. R., Nawaz, R., Young, R., & Coimbra, M. (2020). Gaussian Mixture Model Based Probabilistic Modeling of Images for Medical Image Segmentation. *IEEE Access*, *8*, 16846–16856. https://doi.org/10.1109/ACCESS.2020.2967676

Salman, Y., Gérard, T., Huyghe, L., Colmant, L., Quenon, L., Malotaux, V., Ivanoiu, A., Lhommel, R., Dricot, L., & Hanseeuw, B. J. (2024). Amygdala atrophies in specific subnuclei in preclinical Alzheimer's disease. *Alzheimer's and Dementia*, *20*(10), 7205–7219. https://doi.org/10.1002/alz.14235

Scheltens, P., De Strooper, B., Kivipelto, M., Holstege, H., Chételat, G., Teunissen, C. E., Cummings, J., & van der Flier, W. M. (2021). Alzheimer's disease. In *The Lancet* (Vol. 397, Number 10284, pp. 1577–1590). Elsevier B.V. https://doi.org/10.1016/S0140-6736(20)32205-4

Schumacher, J., Teipel, S., & Storch, A. (2025). Association of Alzheimer's and Lewy body disease pathology with basal forebrain volume and cognitive impairment. *Alzheimer's Research and Therapy* , *17*(1). https://doi.org/10.1186/s13195-025-01678-x

Sorour, S. E., El-Mageed, A. A. A., Albarrak, K. M., Alnaim, A. K., Wafa, A. A., & El-Shafeiy, E. (2024). Classification of Alzheimer's disease using MRI data based on Deep Learning Techniques. *Journal of King Saud University - Computer and Information Sciences*, *36*(2). https://doi.org/10.1016/j.jksuci.2024.101940

Tran, T. T., Speck, C. L., Gallagher, M., & Bakker, A. (2022). Lateral entorhinal cortex dysfunction in amnestic mild cognitive impairment. *Neurobiology of Aging*, *112*, 151–160. https://doi.org/10.1016/j.neurobiolaging.2021.12.008

Truong Thanh Nguyen, H., Vo Thanh Nguyen, K., & Dinh Khoi Pham, N. (2021). *Evaluation of Explainable Artificial Intelligence: SHAP, LIME, and CAM Hung Quoc Cao*.

Vimbi, V., Shaffi, N., & Mahmud, M. (2024). Interpreting artificial intelligence models: a systematic review on the application of LIME and SHAP in Alzheimer's disease detection. In *Brain Informatics* (Vol. 11, Number 1). Springer Science and Business Media Deutschland GmbH. https://doi.org/10.1186/s40708-024-00222-1

Wijeratne, T., Andrade-Guerrero, J., Santiago-Balmaseda, A., Jeronimo-Aguilar, P., Vargas-Rodríguez, I., Ruth Cadena-Suárez, A., Sánchez-Garibay, C., Pozo-Molina, G., Fabiola Méndez-Catalá, C., Cardenas-Aguayo, M.-C., Diaz-Cintra, S., Pacheco-Herrero, M., Luna-Muñoz, J., & Soto-Rojas, L. O. (2023). Citation: Alzheimer's Disease: An Updated Overview of Its Genetics. *Int. J. Mol. Sci*, *2023*, 3754. https://doi.org/10.3390/ijms

Xie, L., Wisse, L. E. M., Das, S. R., Vergnet, N., Dong, M., Ittyerah, R., de Flores, R., Yushkevich, P. A., & Wolk, D. A. (2020). Longitudinal atrophy in early Braak regions in preclinical Alzheimer's disease. *Human Brain Mapping*, *41*(16), 4704–4717. https://doi.org/10.1002/hbm.25151

Xu, J., Wang, S., Yang, D., Huang Chuah, J., Wee Lai, K., Bao, W., & C-o, C. (2023). *Conventional machine learning and deep learning in Alzheimer's disease diagnosis using neuroimaging: A review*.

Yajjala, A., Ravi, A., & Bhanu Chander, G. (2025). Optimizing Multi-Class Fault Detection in Digital Circuits Using a Hybrid Ensemble of Random Forest and XGBoost. *Proceedings of 2025 International Conference on Emerging Trends in Industry 4.0 Technologies, ICETI4T 2025*. https://doi.org/10.1109/ICETI4T63625.2025.11132202

Zhou, J., Wan, J., Chen, X., Li, X., Wu, Z., Zhang, Z., & Zhang, C. (2026). ViViMZheimer a slice based end to end model for Alzheimer's disease diagnosis from 3D MRI. *Scientific Reports*, *16*(1). https://doi.org/10.1038/s41598-025-29119-7